

The ancestral *C. elegans* cuticle suppresses *rol-1*

Luke M. Noble^{1,2,3}, Asif Miah², Taniya Kaur² and Matthew V. Rockman^{2,3}

¹Institut de Biologie, École Normale Supérieure, CNRS 8197, Inserm U1024, PSL Research University, F-75005 Paris, France, ²Center for Genomics and Systems Biology, Department of Biology, New York University, New York, NY, 10003, USA

ABSTRACT Genetic background commonly modifies the effects of mutations. We discovered that worms mutant for the canonical *rol-1* gene, identified by Brenner in 1974, do not roll in the genetic background of the wild strain CB4856. Using linkage mapping, association analysis and gene editing, we determined that N2 carries an insertion in the collagen gene *col-182* that acts as a recessive enhancer of *rol-1* rolling. From population and comparative genomics, we infer the insertion is derived in N2 and related laboratory lines, likely arising during the domestication of *Caenorhabditis elegans*, and breaking a conserved protein. The ancestral version of *col-182* also modifies the phenotypes of four other classical cuticle mutant alleles, and the effects of natural genetic variation on worm shape and locomotion. These results underscore the importance of genetic background and the serendipity of Brenner's choice of strain.

KEYWORDS genetic background; genetic interaction; cuticle; collagen

Introduction

Since Morgan's first white-eyed fly, forward genetics has been one of our most powerful tools for discovering biological mechanisms. In 1974, Sydney Brenner introduced geneticists to *C. elegans*, an experimental organism with properties ideal for probing the molecular basis of development and neurobiology (Brenner 1974). Brenner began by isolating mutants with conspicuous effects under the evocative nomenclature of Dumpy, Squat, Long, Blistered, and Roller phenotypes, including a single allele of *rol-1*. This mutation causes helical twisting of the adult worm's cuticle, which manifests most obviously as sinusoidal motion along the short axis of locomoting animals and consequent gyration on the uniform surface of an agar plate.

rol-1, and several other genes from Brenner's first screen, opened the door not only to linkage mapping in *C. elegans* but also to decades of productive work on the worm cuticle. The cuticle is a complex structure, made primarily of cross-linked collagens generated anew with each larval molt (Page and Johnstone 2007). It plays an integral structural role as both barrier and morphological scaffold for muscle attachment. Epistasis analysis of collagens and collagen-modifying enzymes represents a landmark example of the power of transmission genetics to reveal molecular and developmental mechanisms (Higgins and Hirsh 1977; Cox *et al.* 1980; Kramer and Johnson 1993; McMahon *et al.* 2003).

Brenner's original screen, and the vast majority of subsequent research in *C. elegans*, took place in the genetic context of the inbred reference strain, N2. Over the past decade, researchers

have discovered that N2 evolved during its adaptation to laboratory conditions, and that wild isolates of *C. elegans* differ from the lab strain in diverse and substantive ways (Hodgkin and Doniach 1997; de Bono and Bargmann 1998; McGrath *et al.* 2009; Duveau and Félix 2012; Andersen *et al.* 2014; Sterken *et al.* 2015; Large *et al.* 2016; Gimond *et al.* 2019). Critically, the effects of mutations are often modified by genetic background. This kind of background dependence both complicates experimental analyses and underlies important genetic phenomena such as variable penetrance of Mendelian diseases in humans (Summers 1996; Scriver and Waters 1999; Dipple and McCabe 2000; Gibson and Dworkin 2004; Paaby and Rockman 2014; Paaby and Gibson 2016).

While using a *rol-1* allele as a visible marker for genetic mapping experiments, we discovered that its rolling phenotype is substantially suppressed by a wild strain background. We mapped the major-effect locus responsible for this suppression, finding that N2 carries a derived insertion in *col-182*, a collagen gene with no known mutational effects. The ancestral allele of this collagen, found in all wild isolates of *C. elegans* and highly conserved among *Caenorhabditis* species, also modifies the effects of other canonical cuticle mutants, including those with Blistered and Squat phenotypes. These results underscore the importance of genetic background and the serendipity of Brenner's choice of strain.

³L. M. Noble, noble@biologie.ens.fr; M. V. Rockman, mrockman@nyu.edu

1 Materials and Methods

2 Strains

3 All experiments were carried out at 20° with NGM-agarose
4 plates and OP50-1 *E. coli* for food, unless otherwise noted.

5 We used the following strains: BE8: *sqt-3(sc8)* V, BE13: *sqt-*
6 *1(sc13)* II, BE22: *rol-1(sc22)* II, BE44: *dpy-8(sc44)* X, BE93: *dpy-*
7 *2(e8)* II, BE108: *sqt-2(e108)* II, CB61: *dpy-5(e61)* I, CB91: *rol-*
8 *1(e91)* II, CB224: *dpy-11(e224)* V, CB768: *bli-2(e768)* II, CB769:
9 *bli-1(e769)* II, CB1166: *dpy-4(e1166)* IV, CB2070: *bli-1(e935) rol-*
10 *1(e91)* II, CB4856: Hawaiian wild type, COP1834: *col-182(knu732)*
11 X, EG7993: *oxTi412 [left-3p::TdTomato::H2B]* X, EG8951: *oxTi1015*
12 *[left-3p::GFP::NLS + NeoR]* X, N2: laboratory wild type, QG2797:
13 *rol-1(e91)* II; *ajIR6 [X, CB4856 > N2]* X, QG2798: *rol-1(e91)*
14 II; *oxTi412 [left-3p::TdTomato::H2B] oxTi1015 [left-3p::GFP::NLS*
15 *+ NeoR]* X, QG2804: *mIs12 rol-1(e91)* II, QG2952: *bli-1(e769)*
16 II; *col-182(knu732)* X, QG2954: *dpy-11(e224)* V; *col-182(knu732)*
17 X, QG2953: *rol-1(e91)* II; *col-182(knu732)* X, QG2955: *dpy-*
18 *4(e1166)* IV; *col-182(knu732)* X, QG2956: *bli-1(e935) rol-1(e91)*
19 II; *col-182(knu732)* X, QG2957: *rol-1(sc22)* II; *col-182(knu732)* X,
20 QG2958: *dpy-2(e8)* II; *col-182(knu732)* X, QG2960: *dpy-5(e61)*
21 I; *col-182(knu732)* X, QG2961: *sqt-2(e108)* II; *col-182(knu732)* X,
22 QG2962: *bli-2(e768)* II; *col-182(knu732)* X, QG3070: *sqt-3(sc8)*
23 V; *col-182(knu732)* X, QG3072: *sqt-1(sc13)* II; *col-182(knu732)* X,
24 QG3074: *dpy-10(cn64)* II; *col-182(knu732)* X, QG3076: *dpy-8(sc44)*
25 *col-182(knu732)* X, SP419: *unc-4(e120) rol-1(e91)* II, TN64: *dpy-*
26 *10(cn64)* II, and WE5241: *ajIR6 [X, CB4856 > N2]* X. COP1834
27 was generated by Knudra Biosciences (now NemaMetrix).

28 We verified the presence of the *rol-1(e91)* mutation in these
29 strains by Sanger sequencing using primers RolF3: CAAATTC-
30 GACAAAGCGACAA and RolR3: GAGCATCGTAAGGCTG-
31 GAAA. We verified the presence of the *col-182(knu732)* mu-
32 tation by Sanger sequencing using primers X12.636F: TAG-
33 GCAAACCTTGCTGCACAC and X12.636R: GAGACAGGCTG-
34 GAAATGAGC.

35 Observation of segregation distortion

36 As described in Kaur and Rockman (2014), we crossed wild
37 isolate CB4856 and a strain carrying *unc-4(e120) rol-1(e91)* II in
38 the N2 background. *F*₁ hermaphrodites were singled and Rol
39 nonUnc *F*₂ adults were isolated and genotyped by Illumina
40 GoldenGate Assay. Genotyping was performed by the DNA
41 Sequencing and Genomics Core Facility of the University of
42 Utah. Allele frequencies are in File S2.

43 Complementation crosses

44 We used visible markers to generate animals that are homozy-
45 gous *rol-1* on chromosome II and heterozygous on the X chromo-
46 some, with one X chromosome from N2 and the second from the
47 strain of interest (SOI). If the SOI carries the dominant suppress-
48 or of *rol-1*, then these animals are expected to show suppressed
49 rolling behavior.

50 Specifically, we crossed *mIs12[GFP] rol-1* II males to SOI
51 hermaphrodites to generate *mIs12 rol-1 / + +* II; SOI X *F*₁ males.
52 These we crossed to *unc-4 rol-1* II hermaphrodites. For each SOI,
53 we tested six GFP-positive nonUnc hermaphrodite progeny of
54 this cross for rolling behavior in the second day of adulthood.
55 These animals are mostly *unc-4 + rol-1 / + mIs12 rol-1* II; SOI/N2
56 X. A small fraction of the phenotyped animals could be *rol-1*
57 heterozygotes due to rare recombination events between *mIs12*
58 and *rol-1* in the *F*₁ males. In addition, each tested animal is het-
59 erozygous (N2/SOI) for a random fraction (expectation ½) of
60 the autosomes except for chromosome II.

We also tested 8 wild isolates by this approach (CB4856, 61
PB306, EG4347, QX1211, JU319 [CeNDR isotype JU311], JU1088, 62
PX179, and JU400 [CeNDR isotype JU394]), along with N2 and 63
LJS1, which are laboratory-adapted strains. 64

65 Fine mapping with recombinants

66 To fine-map the suppressor, we crossed *rol-1(e91)* II; CB4856 X
67 and *rol-1(e91)* II; *oxTi1015 oxTi412* X. The latter strain carries
68 integrated single-copy transgenes on the X expressing fluore-
69 scent proteins, tdTomato::H2B from X:11.049 Mb and GFP::NLS
70 from X:13.480 Mb [Wormbuilder; Frøkjær-Jensen *et al.* (2014)].
71 Both strains carry N2-derived autosomes. We homozygosed X
72 chromosomes that were recombinant between the transgenes,
73 scored their rolling behavior, and genotyped them at SNP mark-
74 ers in the mapping interval. Recombinant strain AM_GNR9
75 placed the suppressor to the right of SNP WBVar00083599 at
76 X:12,579,121, and recombinant AM_GNR13 placed it to the left
77 of SNP WBVar1602269 at X:12,662,633.

78 Genotyping primers used for mapping were: WB-
79 Var01981458 indel, TGGGTAACATCGGCTCCAT and
80 TGTTCTGCACGGGAAAAGAT; WBVar00083599 SNP,
81 CGACATCCAAAGTTTTTGAGACT and GAGAAAGTGT-
82 TATGGGCATGG; WBVar01602269 SNP, CGTGTGTTTC-
83 CGTTGTGAAT and TTCAGTGTTCATCGCAATCTG.

84 Association mapping

85 Variant data for 330 *C. elegans* isotypes were downloaded as
86 the 20180527 CeNDR release soft-filtered vcf. We tested for a
87 match between variants in the recombination-mapping interval
88 (X:12,579,122 - X:12,662,632) and *rol-1* suppression phenotypic
89 in the panel of N2, CB4856, LSJ1, and the seven other tested wild
90 isolates.

91 Gene model

92 Sequence and annotation data for the *Caenorhabditis* genus were
93 downloaded from the *Caenorhabditis* Genomes Project. RNAseq
94 data from young adults of *C. elegans* wild isolates were down-
95 loaded from the NCBI SRA: CB4856 PRJNA437313 (Zamanian
96 *et al.* 2018), AB1 and ED3040 PRJNA288824 (Vu *et al.* 2015). Reads
97 were mapped to a 100 Kb region of the N2 WS220 genome cen-
98 tered on *col-182* with bwa mem version 0.7.17 (Li and Durbin
99 2010), assembled with Trinity version 2.3.2 in genome-guided
100 mode (Grabherr *et al.* 2011), and homologous transcripts were
101 extracted by blast version 2.9 (Altschul *et al.* 1990) against *col-182*
102 orthologs across the genus. Coding and protein sequences were
103 aligned with mafft version 7.3.10 in L-INS-i mode (Katoh *et al.*
104 2005), and homology and gene structures were plotted using R
105 packages *ape* (Paradis and Schliep 2019), *ggtree* (Yu *et al.* 2017),
106 *Biostrings* (Pagès *et al.* 2019), and *ggbio* (Yin *et al.* 2012). Species
107 with only computationally predicted annotations (*C. kamaaina*,
108 *C. becei*, *C. panamensis*) and two species (*C. quiockensis* and *C. sul-*
109 *stoni*) with extremely long predicted ortholog sequences poten-
110 tially deriving from annotation errors were excluded. Collagen
111 triplet stability scores shown in Figure 2B were obtained from
112 (Persikov *et al.* 2005), and ignore higher-order interactions. Gene
113 models and coding sequence alignments are in Files S10,S11.

114 Epistasis analysis of visible mutants

115 For each tested mutation, we grew the mutant line and *col-*
116 *182(knu732)* double mutant in parallel at low population den-
117 sities for several generations and performed synchronous egg
118 lays to generate animals for phenotyping. For most strains we

1 observed these synchronized animals three days later as young
2 adults. For *sqt-2(sc108)*, because the heterozygous phenotype
3 (Rol) is different from the homozygous phenotype (Sqt), we also
4 scored *sqt-2/+* animals. For *rol-1 bli-1* and *rol-1 bli-1; col-182* ani-
5 mals, we followed 200 of each genotype through the third day
6 of adulthood. Videos of *rol-1* worms (CB91, QG2979, QG2957,
7 BE22, QG2953) were taken on day four of adulthood. Ten worms
8 were picked to fresh seeded plates and imaged for 8 minutes at
9 12 frames per minute. Videos of *sqt-3* worms (BE8, QG3070) were
10 taken on day two of adulthood. Twenty worms were picked to
11 fresh seeded plates and imaged for five minutes at 12 frames per
12 minute. Video samples are in Files S3-S9.

13 **Quantitative locomotion analysis**

14 Conditions and worm tracking have been described previously
15 (Noble *et al.* 2017; Mallard *et al.* 2019). Lines (N2, COP1834, BE8,
16 BE22, QG2957, QG3070) were each split to duplicate lineages,
17 bleached, and grown under common conditions on HT115 bacte-
18 ria in 90mm plates at 20° for two generations before assay, with
19 each generation starting from around 500 L1 larvae that had
20 been starvation synchronised in M9 buffer for 18 hours. Young
21 adults were imaged in random order, on food, during day three
22 post-L1, and again on two further generations (treated as above)
23 for a total of six replicate plates per genotype. Worms were
24 tracked for 8 minutes using the Multi-Worm Tracker (Swierczek
25 *et al.* 2011), the final 4 of which were analysed after subsampling
26 to 4 Hz, and 11-point skeletons and outlines from Choreography
27 were parsed to generate summary track statistics based on size
28 and movement. More precisely, we used Choreography-defined
29 measurements of length, width, area, speed, acceleration, angu-
30 lar momentum (turning rate), mean body curvature, kink (the
31 maximum ratio of angles between head/tail and body), and the
32 length of continuous runs of Forward, Backward or Still motion
33 (“bias”). Raw data are in File S12.

34 For each worm track we took the median and variance of each
35 metric, as a whole and split by bias state. Exploratory behaviour
36 was quantified as the area and circularity ($4\pi \text{ area} / \text{perimeter}^2$)
37 of the track convex hull (Pebesma and Bivand 2005), averaged
38 first across 30 second intervals for each of the longest 100 tracks
39 from each plate, then across tracks. Traits were log transformed
40 where strongly non-normal (an improvement in Shapiro-Wilk
41 $-\log_{10}$ p-value > 6), and effects of assay block, defined by lineage
42 and assay day, were removed by linear regression. Processed
43 data are in File S13.

44 We show univariate and multivariate (classical multidimen-
45 sional scaling on the mean centered and scaled Euclidean dis-
46 tance matrix of plate means, base R *cmdscale*) analysis. In Fig-
47 ure 3A-B we used multivariate analysis of a subset of seven
48 traits selected using sparse linear discriminant analysis (Clem-
49 mensen *et al.* 2011). From 25 traits (repeatability > 0.5, thinned
50 to reduce maximum colinearity to $r^2 < 0.5$), we selected the five
51 metrics most associated with suppression of *rol-1(sc22)* or *sqt-*
52 *3(sc8)*, separately, using plate means. Traits retained for *sqt-3*
53 (BE8 vs. QG3070, COP1834, N2), ordered by absolute loading on
54 the discriminant function, were log transformed curvature (S),
55 width (F), kink, width (S) variance, and acceleration (F). Traits
56 retained for *rol-1* (BE22 vs. QG2957, COP1834, N2) were log
57 transformed circularity, velocity variance, width (F), kink (F),
58 and run length (F) variance. R code for this analysis is in File
59 S14.

Epistasis analysis in the CeMEE

To test for potential modifying effects of *col-182* on natural vari-
61 ation segregating in the *C. elegans* multiparent experimental
62 evolution (CeMEE) panel we genotyped the N2 indel from exist-
63 ing sequence data (Noble *et al.* 2019) using bcftools (Li 2011)
64 after indel realignment (DePristo *et al.* 2011), obtaining calls for
65 365 recombinant inbred lines (RILs; from populations A6140,
66 CA[1-3]50 and GA[1,2,4]50) for which locomotion has been mea-
67 sured on NGM (Mallard *et al.* 2019). Two lines were excluded
68 as multivariate outliers based on Mahalanobis distance. Geno-
69 types were marker set 1 from Noble *et al.* (2019). The N2 *col-182*
70 allele is at a frequency of 16.5% in these lines, providing suffi-
71 cient power to detect pairwise interactions conditional on joint
72 allele frequency. In total, 167,187 diallelic SNPs where all four
73 genotype classes were present at a minimum frequency of 10,
74 excluding any uncertain imputations, were tested. 75

To test for *col-182*-by-genotype interactions we fit nested bi-
76 variate linear models for three pairs of partially correlated traits:
77 length and width (forward state, log transformed), the *rol-1* and
78 *sqt-3* suppression discriminant functions that are linear combi-
79 nations of five traits (see Quantitative locomotion analysis), and
80 the single traits with the highest loading in each discriminant
81 function, curvature and track circularity (log transformed). Trait
82 values were best linear unbiased predictions (BLUPs) extracted
83 from linear mixed effects models (R package *lme4*) fit to replicate
84 observations, with fixed effects of population replicate. Signifi-
85 cance testing followed the univariate approach in Noble *et al.*
86 (2017). In brief, we first tested for genetic effects by likelihood
87 ratio (Pillai’s trace statistic) for a full model, with additive and in-
88 teraction effects of *col-182* genotype and focal marker genotype,
89 against a null model (intercept only). Genome-wide significance
90 was declared against a null distribution of >1000 test statistics
91 generated by permuting lines within populations and retaining
92 the minimum observed *p*-value. We used a relative permissive
93 false discovery rate (FDR) of 0.2. Quantile-quantile plots showed
94 statistics were well calibrated for length/width and the Rol/Sqt
95 discriminant functions at $p > 10^{-3}$, but strongly deflated for
96 curvature/circularity. Inflation was evident for length/width
97 at $p < 10^{-3}$, independent of linkage disequilibrium, consistent
98 with additional polygenic interactions. For loci with significant
99 genetic effects, interaction significance was then assessed at a
100 nominal threshold of $p < 0.05$ by parametric bootstrap against
101 the additive model (Bůžková *et al.* 2011), resampling responses
102 jointly among lines 5000 times. Genotype and phenotype data,
103 and R code for this analysis are in Files S15,S16. 104

Gene expression analysis

We extracted data for 199 recombinant inbred advanced inter-
106 cross lines (RIAILs) from Rockman *et al.* (2010), after exclud-
107 ing data from lines with annotation issues (Zych *et al.* 2017).
108 We performed structured nonparametric trait mapping as in
109 Rockman and Kruglyak (2009) for abundance of 15,617 trans-
110 cripts whose genes are more than a megabase from *col-182*
111 (to exclude local linkages for genes near *col-182* that have their
112 own *cis*-acting variants). We retained traits with genome- and
113 experiment-wide significant linkage peaks (LOD>4.3, 5% FDR)
114 within 1 RIAIL-effective cM of *col-182* (approximately 400 Kb).
115 The nine significantly linked transcripts were tested for func-
116 tional enrichment using the WormBase Enrichment Analysis
117 Suite (Angeles-Albores *et al.* 2018). 118

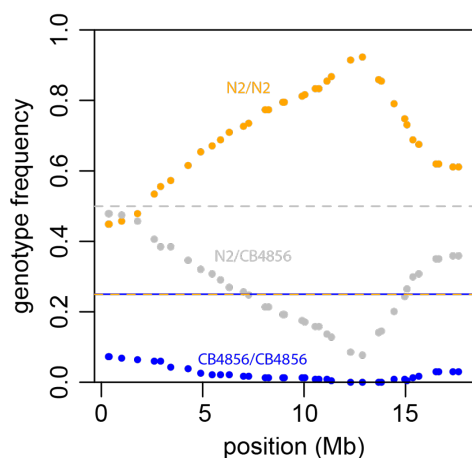
1 Data Availability

2 All quantitative data and code to reproduce our analyses
3 and main figures are available from FigShare (XXX) and
4 github.com/lukemn/cuticle. Strains are available upon request.
5 File S1 details all supplemental files, File S2 contains genotyping
6 data from Figure 1, Files S3-S9 contain short videos of mutant
7 and suppressed adult hermaphrodites on plates, File S10 con-
8 tains gene models from Figure 2A, File S11 contains coding
9 sequence alignments for Figure 2B, Files S12 and S13 contain
10 raw and processed Multi-Worm tracker data for Figure 3 with
11 associated R code in File S14. File S15 contains genotypes and
12 phenotypes used for detecting genetic interactions between *col*-
13 *182* and SNPs in the CeMEE (Figure 4), with associated R code
14 in File 16.

15 Results

16 CB4856 carries a dominant suppressor of *rol-1*

17 During a study of recombination patterns on *C. elegans* chro-
18 mosome II (Kaur and Rockman 2014), we crossed *unc-4(e120)*
19 *rol-1(e91)* II worms (N2 background) with wild isolate strain
20 CB4856, isolated in Hawaii in 1972 (Hodgkin and Doniach 1997).
21 After allowing F_1 hermaphrodites to reproduce by selfing, we
22 isolated Rol nonUnc recombinants, which are homozygous for
23 the N2 *rol-1* allele but carry at least one CB4856 allele at *unc-4*
24 and should show Mendelian segregation of other chromosomes
25 (pace the *peel-1 zeel-1* incompatibility on chromosome I (Seidel
26 et al. 2008)). We noticed strong segregation distortion on the X
27 chromosome among Rol nonUnc recombinants, which we had
28 genotyped at 37 SNP markers (Figure 1, File S2). Distortion
29 favored the N2 background, with a peak around 13 Mb where
30 zero of 234 worms were homozygous for the CB4856 genotype
31 (expectation $\frac{1}{4} = 58.5$). At the peak, 216 (92%) worms were N2
32 homozygotes and the remaining 18 (8%) were heterozygotes.



33 **Figure 1** Allele frequencies along the X chromosome in Rol
34 nonUnc F_2 s from a cross of CB4856 and N2-background *unc*-
35 *4(e120)* *rol-1(e91)* II. Dashed lines show the Mendelian expecta-
36 tions for heterozygotes ($\frac{1}{2}$) and homozygotes ($\frac{1}{4}$ each).

37 We hypothesized that the CB4856 X chromosome carries a
38 dominant suppressor of *rol-1*. We crossed the *rol-1(e91)* allele
39 into an X-chromosome substitution strain, which carries the
40 CB4856 X chromosome but is otherwise N2, and confirmed that
41 the resulting *rol-1(e91)* II CB4856 X strain is strongly, but incom-
42 pletely, suppressed for rolling. The worms retain a slight helical

43 twist and can be distinguished from wildtype N2 and CB4856,
44 but the dramatic rolling and circling behaviors of *rol-1(e91)* are
45 absent (Videos: CB91 vs. QG2797 in Files S3,S4). Suppression of
46 *rol-1* is also observed in X chromosome heterozygotes, consistent
47 with a dominant suppressor on the CB4856 X and explaining the
48 pattern of segregation distortion we observed in the *unc-4 rol-1*
49 crosses.

50 Suppression often reveals interactions between genes in phys-
51 ical association or in specific developmental pathways, but can
52 also reflect altered transcription, splicing, or translation of a mu-
53 tant gene. These informational suppressors can be allele specific,
54 masking only particular kinds of missense or nonsense or splice
55 site variants, for example (Hodgkin 2005). There are two *rol-1* al-
56 leles with known effects on phenotype at present, and we found
57 that the second, *sc22*, is also suppressed by the CB4856 X chro-
58 mosome. Although the *sc22* molecular lesion is unknown, *e91*
59 and *sc22* mutants show distinct phenotypic profiles, including
60 temperature sensitivity (Cox et al. 1980), and we concluded that
61 allele-specific interaction was thus unlikely.

58 The suppressor maps to an indel polymorphism in *col-182*

59 We performed complementation testing with a panel of N2-
60 CB4856 recombinant inbred advanced intercross lines (Rockman
61 and Kruglyak 2009) with breakpoints near the peak allele fre-
62 quency distortion, taking advantage of the dominant mode of
63 action of the CB4856 allele. Using this approach, we tested 5
64 RIAILs, scoring based on Rolling, with boundaries defined by
65 RIAIL QX43, which carries the suppressor, and RIAIL QX126,
66 which does not. These strains place the suppressor to the right
67 of SNP WBVar00083496 at X:12,364,484 and to the left of indel
68 WBVar01981458 at X:12,699,819 (WS272 coordinates).

69 Next we used integrated single-copy fluorescent marker
70 transgenes (Frøkjær-Jensen et al. 2014) to select for N2/CB4856
71 recombinants in the interval, in N2 autosomal genetic back-
72 grounds. These data localized the causative locus to the interval
73 between 12.579 and 12.662 Mb.

74 Complementation testing with seven additional wild isolates
75 found that all exhibit suppression of *rol-1*. Laboratory strain LSJ1,
76 which shares a laboratory ancestor with N2 but was cultured
77 separately since 1963, does not exhibit suppression. Among all
78 variants segregating in these strains in the mapped interval, only
79 one exhibits perfect cosegregation with *rol-1* suppression: an
80 8-base pair (bp) deletion in the gene *col-182* (WBVar01928355).
81 Like *rol-1*, *col-182* is one of the 181 collagen genes in the *C. elegans*
82 genome (Teuscher et al. 2019).

83 N2 carries a derived insertion mutation in *col-182*

84 Among 330 genome-sequenced *C. elegans* isotypes from around
85 the world (CeNDR freeze 20180527), the 8-bp deletion is present
86 in every strain except for the lab strains N2, LSJ1, and ECA252.
87 These three strains are all derived from a single isolate of *C.*
88 *elegans* sampled by L. N. Staniland in 1951 (McGrath et al. 2009;
89 Weber et al. 2010; Sterken et al. 2015; Cook et al. 2017). The
90 deletion state is also found in orthologs of all other examined
91 *Caenorhabditis* species (Figure 2). This strongly suggests the
92 reference allele is a derived insertion, one that arose either in the
93 wild, and happened to be sampled by Staniland in 1951, or in
94 the lab sometime before 1963 [likely before 1958 (Gimond et al.
95 2019)].

96 *C. elegans* collagens contain two blocks of Gly-X-Y repeats,
97 flanked and separated by short cysteine-containing domains
98 involved in interchain disulphide bonds (Page and Johnstone

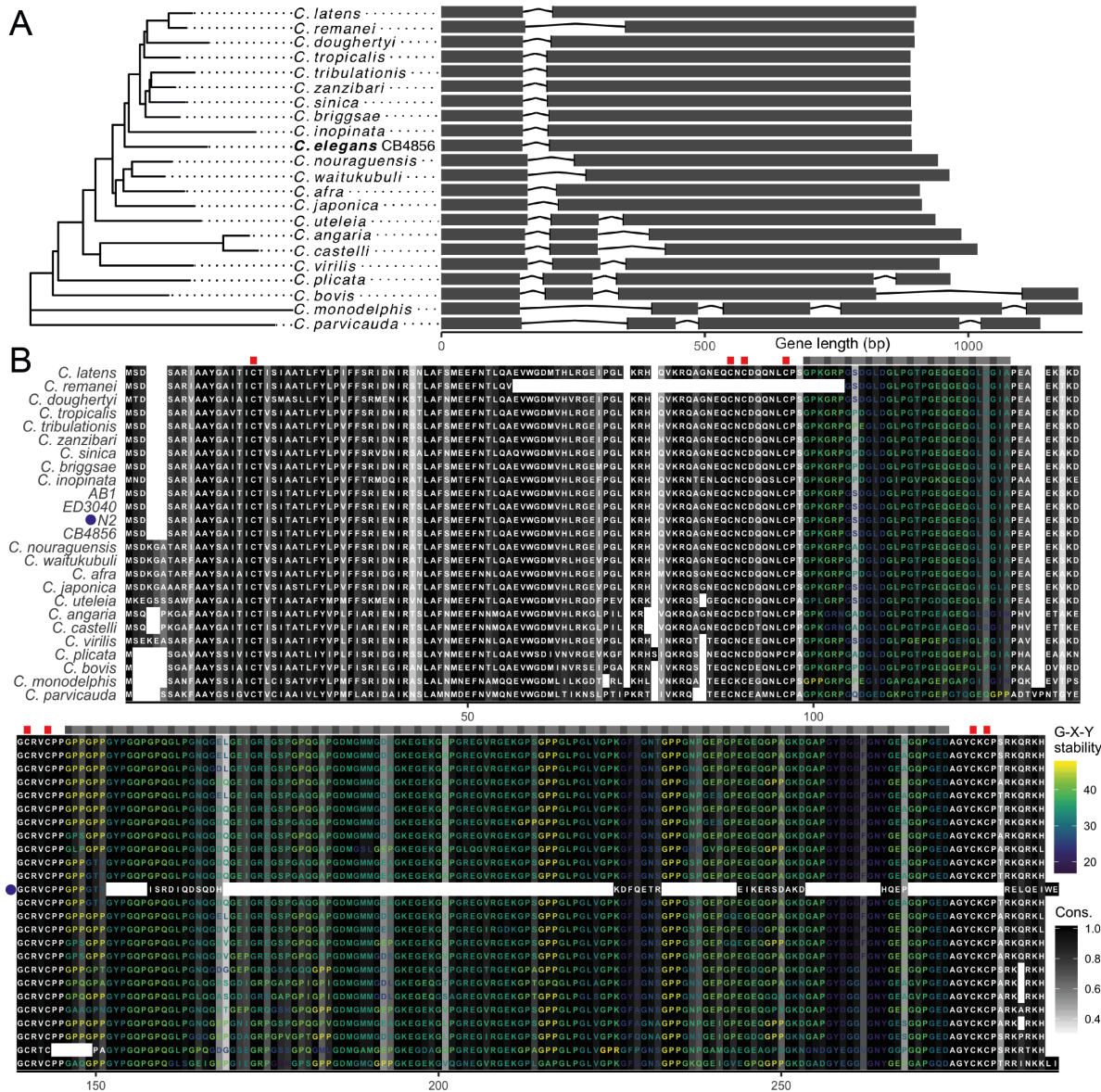


Figure 2 A. *col-182* gene tree and model for *C. elegans* CB4856 and other *Caenorhabditis* species. The x-axis shows distance from the start codon for each genome. **B.** Protein alignment, including predicted sequences for *C. elegans* wild isolates CB4856, AB1 and ED3040 assembled from young adult RNAseq data, and the frame-shifted N2 translation (marked with a blue dot). Grey-scale shading represents site conservation (% identity), and labels are colored by predicted collagen triplet stability (melting temperature) for runs of >1 G-X-Y repeats conserved across all sequences other than N2. The positions of conserved triplets are indicated above the alignment by grey boxes, and the positions of conserved cysteine residues potentially involved in inter-strand disulphide bridges are shown as red boxes.

2007). Until recently, *col-182* was annotated as a three-exon, two-intron gene encoding a near-canonical collagen protein, missing only the middle cysteine domain (Teuscher *et al.* 2019). However, new RNAseq data suggests that the earlier gene model was erroneous, and that the N2 transcript has only one intron (WormBase WS274). With this RNAseq-supported gene model, the 8-bp insertion causes a frameshift that eliminates the entire second Gly-X-Y domain and final cysteine domain (Figure 2B). As a consequence, *col-182* has been reclassified as a pseudogene. The ancestral version of the gene, preserved in CB4856 and all other wild isolates, encodes a perfect canonical cuticular collagen. The C-terminal Gly-X-Y domain includes 43 consecutive Gly-X-Ys, tying it with four other genes for the longest such collagenous stretch among *C. elegans* collagens [with *col-72*, *col-75*, *col-104*, and *col-113*, none of which have known mutant phenotypes; (Teuscher *et al.* 2019)].

To test whether *col-182* is the *rol-1* suppressor and whether the ancestral allele functions via the predicted isoform, we commissioned a strain that carries the ancestral splicing and reading frame in an otherwise N2 background. CRISPR-Cas9 conversion removed the 8-bp insertion and altered 16 additional base pairs, each a synonymous third codon position change in the predicted ancestral reading frame. We then confirmed that this ancestral allele *col-182(knu732)* suppressed *rol-1*, both the *e91* and *sc22* alleles (videos: CB91 vs. QG2953 and BE22 vs. QG2957, Files S3,S5,S6,S7). From tracking of young adult hermaphrodite worms we derived an array of statistics describing locomotion, size, and shape (Quantitative locomotion analysis). Reduction of this data by multidimensional scaling into two orthogonal axes provided quantitative confirmation that the ancestral *col-182(knu732)* allele strongly, but incompletely, suppresses *rol-1* (Figure 3A). By univariate analysis, double mutants are indistinguishable from non-Rol genotypes for a single metric that captures circling locomotion, but weak to no suppression is the predominant outcome across the correlated set of single traits (Figure 3B).

***col-182* interacts with other collagen mutants**

rol-1 is part of a complex network of collagens and collagen-modifying enzymes that interact genetically, often in quite complex ways (Cox *et al.* 1980; Kusch and Edgar 1986). We therefore expected that the ancestral *col-182* might modify *rol-1*'s epistatic relationships with other genes, and might itself interact with other cuticle-specifying genes.

Blistered mutants, described along with *rol-1* in Brenner's original screen, develop fluid-filled blisters along the adult cuticle (Brenner 1974). In the N2 background, *rol-1* suppresses the blister phenotype of *bli-1* mutants (Cox *et al.* 1980). We found that *rol-1 bli-1; col-182* triple mutants show the expected suppression of rolling but are also unblistered, indicating that *col-182* suppresses *rol-1*'s Rol phenotype but not its suppression of *bli-1*. Moreover, *col-182* modified *bli-1*'s phenotype by itself; blisters were largely suppressed in *bli-1; col-182* double mutant hermaphrodites. Blisters were fewer (23% vs. 92% in young adults, n=40 and 36), and were spatially restricted to the head region. Conversely, *col-182* enhances the blister phenotype of *bli-2* worms; *bli-2* young adults had discrete blisters on their bodies or heads (38/39), but a third of *bli-2; col-182* worms had single blisters that spanned the full length of the animal (9/30). The majority of *bli-2* animals (24/40) had blisters restricted to their heads, versus 7/30 for the *bli-2; col-182* worms. Like *col-182* and *rol-1*, *bli-1* and *bli-2* encode collagens.

Cox *et al.* (1980) identified alleles in several genes that give rise to left-handed rollers, like *rol-1(e91)*. Although we observed no gross phenotypic effect of *col-182* on *dpy-8(sc44)*, *dpy-10(cn64)*, or *sqt-1(sc13)*, we observed partial suppression of rolling in *sqt-3(sc8)*, which we quantified by worm tracking (Figure 3, and see videos: BE8 vs. QG3070, Files S8,S9). Suppression was qualitatively and quantitatively distinct to that of *rol-1*; near complete for the single measure of worm width, but again highly variable and generally weak for other measures of locomotion and morphology (Figure 3B).

sqt-2(sc108) exhibits right-handed rolling as a heterozygote in the N2 background, and did so as well in the *col-182(knu732)* background. However, *sqt-2* heterozygotes showed slowed development in the N2 *col-182* background, while the ancestral allele suppressed the developmental delays. Finally, alleles of several additional genes involved in cuticle development – collagens *dpy-2(e8)*, *dpy-4(e1166)* and *dpy-5(e61)*, and thioredoxin *dpy-11(e224)* – showed no gross phenotypic modification in the *col-182(knu732)* background.

***col-182* modifies effects of natural variation on worm shape and locomotion**

Collagens are known to influence body size (Brenner 1974; Fernando *et al.* 2011; Madaan *et al.* 2018), and our locomotion analysis identified specific axes of worm size, posture and locomotion modified by *col-182* in two genetic backgrounds. We next sought to test more broadly for interactions between *col-182* and natural genetic variation for these traits in the *C. elegans* Multiparent Experimental Evolution (CeMEE) panel, a collection of recombinant inbred lines derived from the pooled standing genetic diversity of 14 wild isolates and two N2-related strains (Teotónio *et al.* 2012; Noble *et al.* 2017, 2019).

We genotyped the N2 insertion in RILs sampled from an ancestral laboratory-adapted population, A6140, and from six populations derived from A6140 that evolved under varying mating system and environment (Noble *et al.* 2017). Using Multi-Worm Tracker data for 363 lines, we fit bivariate linear models for three sets of correlated traits (length and width, body curvature and track circularity, and the Rol/Sqt discriminant functions from Figure 3B) to test for interaction effects. Univariate tests showed that *col-182* genotype had no effect on the means of these population-centred traits ($0.37 < p < 0.76$ by likelihood ratio test).

We detected four loci with significant genetic effects at a per-model false discovery rate of 20% (Figure 4). Two QTL were detected for length/width with clear genetic interactions ($p < 0.001$ by bootstrap against the additive model): the first, on chromosome I, fell within the central recombination rate domain (1.5 LOD drop interval around 170 Kb); the second, on chromosome II, was contained by a single very large N2 protein coding gene, *tbc-17*, with several missense variants, a splice-donor change, and heterozygous SNP calls suggestive of copy number variation segregating in the CeMEE founder haplotypes (Cook *et al.* 2017). *tbc-17* encodes a highly conserved predicted Rab family GTPase activator which, based on homology, may be involved in intracellular trafficking, a process critically important for collagen secretion from hypodermal cells (Roberts *et al.* 2003; Ackema *et al.* 2013). Two QTL were detected for the Rol/Sqt discriminant functions: one on chromosome II (interaction bootstrap $p < 0.001$; 18 Kb interval) contained nine N2 annotated protein-coding genes of unknown function, mostly of the nematode-specific peptide group E family; the second, on

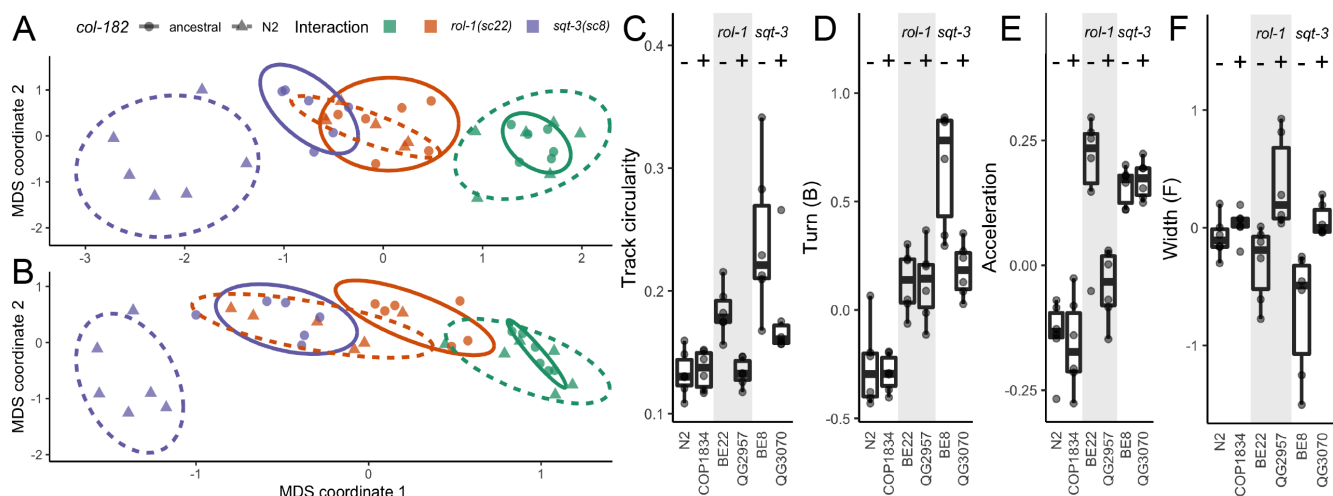


Figure 3 Ancestral *col-182* suppresses *rol-1* and *sqt-3* alleles. **A-B.** Multidimensional scaling of locomotion and size traits: an unbiased set of 19 traits selected only on repeatability across replicate plates (**A**) and a set of seven traits selected by sparse discriminant analysis that maximise multivariate suppression of *sqt-3* or *rol-1* by ancestral *col-182* (**B**). Each point is the grand mean of tracks from around 500 young adult worms per replicate plate over three consecutive generations for each genotype, assayed for N2 (green triangles) and COP1834 (ancestral *col-182* in the N2 background; green circles), BE22 (N2 *col-182*; *rol-1(sc22)*; orange triangles) and QG2957 (ancestral *col-182*; *rol-1(sc22)*; orange circles), and BE8 (N2 *col-182*; *sqt-3(sc8)*; purple triangles) and QG3070 (ancestral *col-182*; *sqt-3(sc8)*; purple circles). **C-F.** Univariate comparisons show variable effects across backgrounds. *col-182* genotype is indicated with - (N2 insertion) and + (ancestral) symbols. Complete suppression of track circularity is seen for *rol-1(sc22)* (**C**), and of worm width in the forward state for *sqt-3(sc8)* (**F**), however partial (or no) suppression is the most common outcome. Raw and processed data in Files S12,S13, code in File S14.

1 chromosome V (interaction $p < 0.02$; 25 Kb interval), was a specific
 2 interaction with MY16 haplotypes, spanning predicted ubiquitin
 3 protease *usp-50* partially, and *dpy-21* fully, along with eight
 4 non-coding RNAs. *dpy-21* is a non-essential, non-condensin
 5 subunit of the dosage compensation (DC) complex (Meyer and
 6 Casson 1986), with additional DC-independent roles in gene
 7 regulation (Webster *et al.* 2013), and loss-of-function mutants
 8 show an enrichment in dysregulation of genes involved in the
 9 cuticle (Kramer *et al.* 2015).

10 ***col-182* does not have systemic effects on gene expression**

11 Several of the alleles that arose during *C. elegans* domestication
 12 have large and systemic effects on *C. elegans* biology. These include
 13 *npr-1* (de Bono and Bargmann 1998; McGrath *et al.* 2009;
 14 Andersen *et al.* 2014; Zhao *et al.* 2018), *nath-10* (Duveau and
 15 Félix 2012), *nurf-1* (Large *et al.* 2016), and *Y17G9B.8* (Rockman
 16 *et al.* 2010; Burga *et al.* 2018). We therefore investigated whether
 17 *col-182* is linked to systemic effects on gene expression in adult
 18 hermaphrodites, using a published dataset of gene expression in
 19 199 N2/CB4856 recombinant inbred advanced intercross lines
 20 [RIAILS; (Rockman *et al.* 2010)]. The RIAILS provide much
 21 higher genotypic replication than a typical pairwise contrast
 22 of strains, as each *col-182* allele is homozygous in approximately
 23 half the RIAILS, but effects that map to *col-182* may be due to
 24 nearby variants in other genes. As expected, *col-182* abundance
 25 shows strong linkage to its own location. Nine other genes show
 26 significant linkage to the *col-182* region Table 1, including two
 27 glutathione S-transferases and two cytochrome P450 enzymes.
 28 However, none are known to be involved in cuticle development
 29 and collectively they show no enrichment for any particular tissue.
 30 Thus the *col-182* mutation in N2 appears to have limited
 31 effects on gene expression in young adult hermaphrodites, at
 32 least under ordinary laboratory conditions.

Probe	ID	Gene	Pos.	Chr.	QTL	LOD
A_12_P107311	R05F9.5	<i>gst-9</i>	4,893,372	2	134.26	8.78
A_12_P120030	B0464.1	<i>dars-1</i>	9,489,112	3	133.00	4.83
A_12_P116084	Y40B10A.2	<i>comt-3</i>	2,061,050	5	133.00	8.62
A_12_P111642	C45H4.17	<i>cyp-33C2</i>	2,186,492	5	134.26	5.34
A_12_P104828	C02A12.1	<i>gst-33</i>	3,467,564	5	133.00	8.50
A_12_P115936	F08F3.7	<i>cyp-14A5</i>	5,421,110	5	133.78	8.56
A_12_P108481	T04H1.9	<i>tbb-6</i>	12,263,208	5	134.26	6.42
A_12_P111217	C05C9.3		11,143,372	6	133.00	4.95
A_12_P105133	C35C5.6	<i>trpp-9</i>	11,569,206	6	133.78	8.13

Table 1 Genes with expression linked to *col-182* in N2/CB4856 RIAILS (Rockman *et al.* 2010). Probe: Agilent microarray probe, ID: WormBase systematic identifier, Gene: common name (if any), Pos./Chr.: physical position of the transcript, QTL: genetic position of the quantitative trait locus in the RIAILS in cM (within 1 cM of *col-182*), LOD: logarithm of the odds of association between gene expression and the QTL peak.

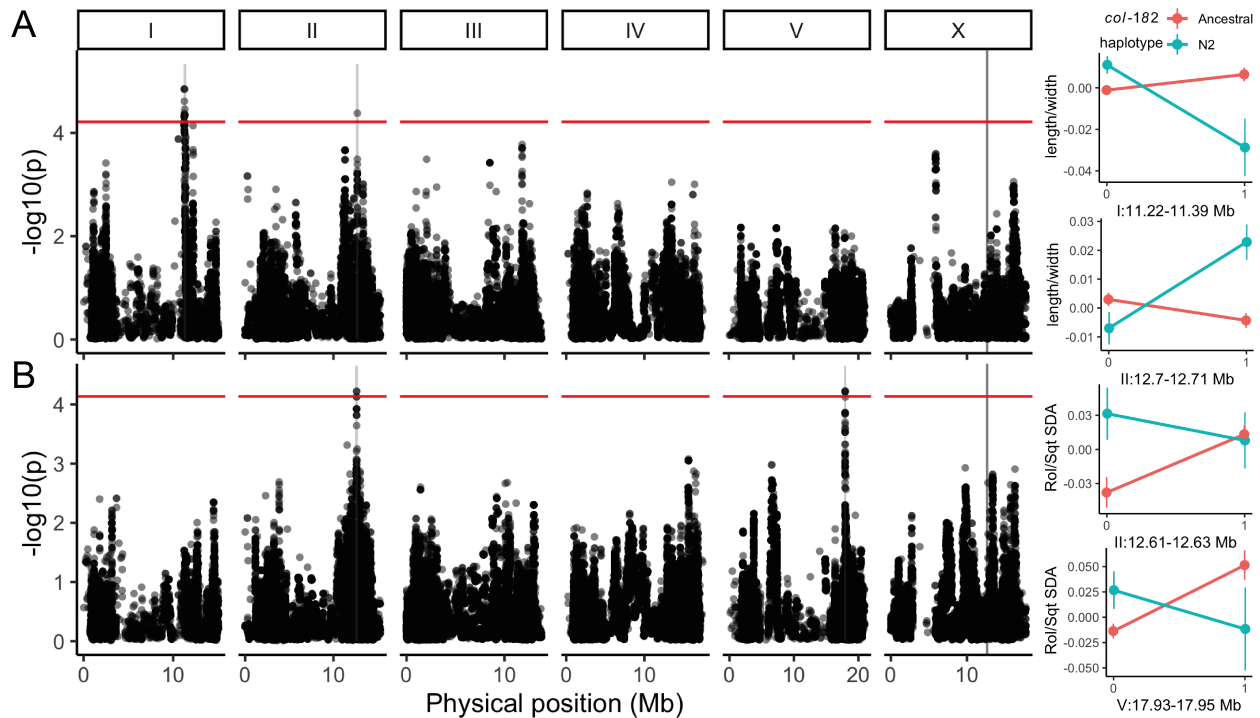


Figure 4 *col-182* modifies the effects of natural genetic variation on worm movement and shape. Genome-wide statistics are shown for two bivariate response models of *col-182* indel \times SNP genotype, worm length/width (A) and Rol/Sqt sparse discriminant functions (B), using diallelic SNPs segregating in 363 recombinant inbred lines of the *C. elegans* multiparent experimental evolution (CeMEE) panel. Statistics are from a likelihood ratio test for a full additive and interaction linear model against a null model of no genetic effects. Permutation thresholds for genome-wide significance (FDR = 0.2) are shown in red, pink shaded regions show 1.5 LOD drop QTL intervals (expanded to a minimum of 300 Kb for visibility), and the location of *col-182* on the X chromosome is indicated by a grey line. Effect plots at right show genotype class means and standard errors for QTL with significant interactions (parametric bootstrap against additive models, $\alpha = 0.05$). Trait values shown are the first principal component for length/width, and the Sqt discriminant function, which explains most of the interaction in the Rol/Sqt bivariate model. Reference-based genotype is on the x-axis. Genotype and phenotype data in File S15, code in File S16.

1 Discussion

2 The structural complexity of the nematode cuticle is reflected in
3 its developmental and genetic regulation, and its environmental
4 (temperature) and genetic sensitivity. Around 4% of the worm
5 genome is dedicated to expressing, processing, and assembling
6 the collagens, cuticulins, glycoproteins and other components
7 of the multilayered extracellular matrix (Teuscher *et al.* 2019).
8 Yet, of 173 predicted cuticular collagen genes, phenotypes from
9 extensive mutagenesis screens have been detected for just 21
10 (Page and Johnstone 2007). To this number we can now add
11 *col-182*, though we have also shown that even this select list
12 might well have been shorter had not Brenner adopted N2 as
13 the *C. elegans* reference genetic background.

14 In the absence of molecular and structural data, the precise
15 role of *col-182* in the worm cuticle and its mode of interaction
16 with other collagens remains obscure. The derived N2 insertion
17 represents an evolved enhancer of *rol-1* rolling, and the ancestral
18 *col-182* modifies to a variable extent the phenotypes from other
19 classical mutant alleles of *bli-1*, *bli-2*, *sqt-2* and *sqt-3*, but not
20 obviously those of *dpy-2*, *-4*, *-5*, *-8*, *-10* and *-11*, or *sqt-1*.

21 The expression of cuticular genes during worm development
22 offers no clear insight. Of the tested genes, only *rol-1*, for which
23 suppression by ancestral *col-182* was strongest, shows strong
24 stage specificity, being around 30-fold enriched in L4 (i.e., when
25 the adult cuticle is manufactured; Figure 5). But *bli-1*, *bli-2* and
26 *rol-1* show generally similar patterns and levels of transcrip-
27 tional activity over the life-cycle, with very low expression in
28 embryonic and early larval stages. The Blistered phenotype is
29 thought to be due to defects in struts linking basal and cortical
30 layers of the adult cuticle, and of six Blistered mutants, three are
31 enzymes rather than structural components.

32 *sqt-1*, *-2* and *-3* are all highly expressed collagens that inter-
33 act genetically, with similar stage specificity from L2 onward
34 (Figure 5). *sqt-3* is unique among collagens in its essentiality
35 (Priess and Hirsh 1986; van der Keyl *et al.* 1994; Novelli *et al.*
36 2006), and is strongly expressed in the embryo as well. *sqt-1* also
37 interacts genetically with *bli-1* and *bli-2*, and 22 other genes (Cox
38 *et al.* 1980; Kusch and Edgar 1986; Kramer and Johnson 1993;
39 Kramer 1994; Westlund *et al.* 1997; Nyström *et al.* 2002; Byrne
40 *et al.* 2007; Shephard *et al.* 2011; Cai *et al.* 2011), yet we saw no
41 obvious modification of the left rolling phenotype of *sqt-1(sc13)*
42 mutants in the ancestral *col-182* background. This may be ex-
43 plained by the extreme specificity of allelic interactions among
44 collagen mutants, and *sqt* mutants in particular. The *sqt-1(sc13)*
45 allele tested is a recessive C-terminal C>Y substitution, altering
46 cross-linking (Kramer and Johnson 1993; Yang and Kramer 1999),
47 while *sqt-2(sc108)* is an N-terminal R>C substitution of unknown
48 structural effect. Alleles of *sqt-1* vary markedly in their type,
49 severity, temperature sensitivity, and degree of dominance of
50 phenotypes, as well as inter- and intragenic interaction effects;
51 from near wild-type for a null allele, to left or right rolling, ab-
52 normal hermaphrodite tail or male rays, or variation in body
53 length. Enrichment in CeMEE interaction statistics for worm
54 length/width over a small region spanning *sqt-1* ($p < 0.00022$)
55 provides some fuel for speculation that allele-specific interac-
56 tions with *col-182* may exist.

57 Lastly, no grossly visible interactions were seen for collagens
58 involved in annuli formation and shape *dpy-2*, *-5*, *-8*, *-10* (McMa-
59 hon *et al.* 2003). In sum, we surmise that *col-182* likely plays
60 a role, apparently redundant under laboratory conditions, in
61 one or both of the strut-anchored adult cuticular layers. The
62 oft-touted genetic simplicity of *C. elegans* breaks down some-

what when considering the cuticle, and targeted biochemical
and structural analysis, together with epistasis analysis encom-
passing natural genetic variation, will be required to clarify the
precise role of *col-182* and the majority of other collagens with
no known function in the N2 background.

Effects of genetic background are ubiquitous in complex ge-
netic systems wherever they are carefully considered. Studies
mixing natural with domesticated genetic variation have amply
shown the importance of genetic interaction on the phenotypic
outcome of allelic effects in *C. elegans* (Seidel *et al.* 2008; McGrath
et al. 2009; Bendesky *et al.* 2012; Duveau and Félix 2012; Gaertner
et al. 2012; Andersen *et al.* 2014; Glater *et al.* 2014; Greene *et al.*
2016; Ben-David *et al.* 2017; Bernstein *et al.* 2018; Zhao *et al.* 2018).
This extends to classical mutations of the cuticle, some of the
first mutants isolated in *C. elegans* and core components of the
worm geneticist's toolkit.

Acknowledgments

This work was supported by the National Science Founda-
tion (DDIG 1210762 to TK), the National Institutes of Health
(R01GM121828 to MVR), the NYU Dean's Undergraduate Re-
search Fund (AM), and the European Commission Sklodowska-
Curie Fellowship (H2020-MSCA-IF-2017-798083 to LMN). For
sharing data and facilities, we thank Henrique Teotónio. For
strains, we thank Erik Andersen and the *Caenorhabditis* Genetics
Center, funded by the NIH Office of Research Infrastructure Pro-
grams (P40 OD010440). We thank Jia Shen, John Yuen, Arielle
Martel, James Hong, and Ambika Natesan for assistance with
experiments.

Literature Cited

- Ackema, K. B., U. Sauder, J. A. Solinger, and A. Spang, 2013 The
ArfGEF GBF-1 Is Required for ER Structure, Secretion and
Endocytic Transport in *C. elegans*. *PLOS ONE* 8: e67076.
- Altschul, S. F., W. Gish, W. Miller, E. W. Myers, and D. J. Lipman,
1990 Basic local alignment search tool. *Journal of Molecular
Biology* 215: 403–410.
- Andersen, E. C., J. S. Bloom, J. P. Gerke, and L. Kruglyak, 2014 A
variant in the neuropeptide receptor *npr-1* is a major determi-
nant of *Caenorhabditis elegans* growth and physiology. *PLOS
Genetics* 10: e1004156.
- Angeles-Albores, D., R. Y. N. Lee, J. Chan, and P. W.
Sternberg, 2018 Two new functions in the Worm-
Base Enrichment Suite. *Micropublication: biology* p. 3,
Dataset. <https://doi.org/10.17912/W25Q2N>.
- Ben-David, E., A. Burga, and L. Kruglyak, 2017 A maternal-effect
selfish genetic element in *Caenorhabditis elegans*. *Science*
(New York, N.Y.) 356: 1051–1055.
- Bendesky, A., J. Pitts, M. V. Rockman, W. C. Chen, M.-W. Tan,
et al., 2012 Long-range regulatory polymorphisms affecting
a GABA receptor constitute a quantitative trait locus (QTL)
for social behavior in *Caenorhabditis elegans*. *PLOS Genetics* 8:
e1003157.
- Bernstein, M. R., S. Zdraljevic, E. C. Andersen, and M. V. Rock-
man, 2018 Tightly-linked antagonistic-effect loci underlie poly-
genic demographic variation in *C. elegans*. *bioRxiv* p. 428466.
- Boeck, M. E., C. Huynh, L. Gevirtzman, O. A. Thompson,
G. Wang, *et al.*, 2016 The time-resolved transcriptome of *C.*
elegans. *Genome Research* 26: 1441–1450.
- Brenner, S., 1974 The Genetics of *Caenorhabditis Elegans*. *Genet-
ics* 77: 71–94.

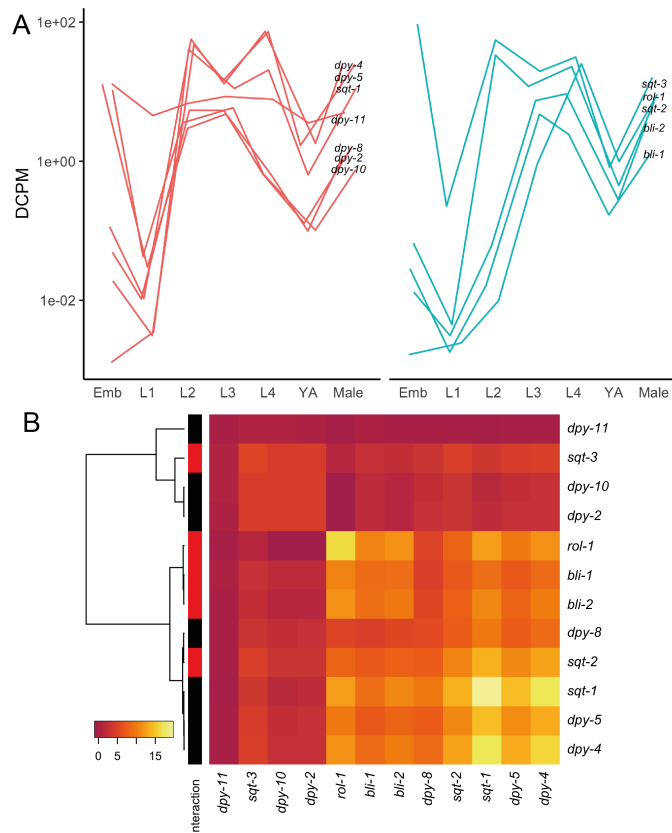


Figure 5 Developmental expression of cuticle genes, mutant alleles of which were tested for genetic interactions with *col-182*. Expression trajectories (A), split by the presence of any detected genetic interaction (*col-182* interactors at right, with a small positional jitter added along the x-axis as a visual aid), and expression covariance (B) across embryonic and larval stages and young adult (YA) hermaphrodites and males. Mean values of replicate experiments per stage are shown from Boeck *et al.* (2016).

- Burga, A., E. Ben-David, T. L. Vergara, J. Boocock, and L. Kruglyak, 2018 Fast genetic mapping of complex traits in *C. elegans* using millions of individuals in bulk. *bioRxiv* p. 428870.
- Byrne, A. B., M. T. Weirauch, V. Wong, M. Koeva, S. J. Dixon, *et al.*, 2007 A global analysis of genetic interactions in *Caenorhabditis elegans*. *Journal of Biology* **6**: 8.
- Bůžková, P., T. Lumley, and K. Rice, 2011 Permutation and parametric bootstrap tests for gene-gene and gene-environment interactions. *Annals of human genetics* **75**: 36–45.
- Cai, L., B. L. Phong, A. L. Fisher, and Z. Wang, 2011 Regulation of Fertility, Survival, and Cuticle Collagen Function by the *Caenorhabditis elegans* *eaf-1* and *ell-1* Genes. *Journal of Biological Chemistry* **286**: 35915–35921.
- Clemmensen, L., D. Witten, T. Hastie, and B. Ersbøll, 2011 Sparse Discriminant Analysis. *Technometrics* **53**: 406–413.
- Cook, D. E., S. Zdraljevic, J. P. Roberts, and E. C. Andersen, 2017 CeNDR, the *Caenorhabditis elegans* natural diversity resource. *Nucleic acids research* **45**: D650–D657.
- Cox, G. N., J. S. Laufer, M. Kusch, and R. S. Edgar, 1980 Genetic and Phenotypic Characterization of Roller Mutants of *Caenorhabditis Elegans*. *Genetics* **95**: 317–339.
- de Bono, M. and C. I. Bargmann, 1998 Natural variation in a neuropeptide Y receptor homolog modifies social behavior and food response in *C. elegans*. *Cell* **94**: 679–689.
- DePristo, M. A., E. Banks, R. Poplin, K. V. Garimella, J. R. Maguire, *et al.*, 2011 A framework for variation discovery and genotyping using next-generation DNA sequencing data. *Nature Genetics* **43**: 491–498.
- Dipple, K. M. and E. R. McCabe, 2000 Phenotypes of patients with "simple" Mendelian disorders are complex traits: thresholds, modifiers, and systems dynamics. *American Journal of Human Genetics* **66**: 1729–1735.
- Duveau, F. and M.-A. Félix, 2012 Role of pleiotropy in the evolution of a cryptic developmental variation in *Caenorhabditis elegans*. *PLoS biology* **10**: e1001230.
- Fernando, T., S. Flibotte, S. Xiong, J. Yin, E. Yzeiraj, *et al.*, 2011 *C. elegans* ADAMTS ADT-2 regulates body size by modulating TGF β signaling and cuticle collagen organization. *Developmental biology* **352**: 92–103.
- Frøkjær-Jensen, C., M. W. Davis, M. Sarov, J. Taylor, S. Flibotte, *et al.*, 2014 Random and targeted transgene insertion in *Caenorhabditis elegans* using a modified Mos1 transposon. *Nature Methods* **11**: 529–534.
- Gaertner, B. E., M. D. Parmenter, M. V. Rockman, L. Kruglyak, and P. C. Phillips, 2012 More than the sum of its parts: a complex epistatic network underlies natural variation in thermal preference behavior in *Caenorhabditis elegans*. *Genetics* **192**: 1533–1542.
- Gibson, G. and I. Dworkin, 2004 Uncovering cryptic genetic variation. *Nature Reviews Genetics* **5**: 681–690.
- Gimond, C., A. Vielle, N. Silva-Soares, S. Zdraljevic, P. T. McGrath, *et al.*, 2019 Natural Variation and Genetic Determinants of *Caenorhabditis elegans* Sperm Size. *Genetics* **213**: 615–632.
- Glater, E. E., M. V. Rockman, and C. I. Bargmann, 2014 Multi-genic natural variation underlies *Caenorhabditis elegans* olfactory preference for the bacterial pathogen *Serratia marcescens*. *G3 (Bethesda, Md.)* **4**: 265–276.
- Graherr, M. G., B. J. Haas, M. Yassour, J. Z. Levin, D. A. Thompson, *et al.*, 2011 Full-length transcriptome assembly from RNA-Seq data without a reference genome. *Nature Biotechnology* **29**: 644–652.

- 1 Greene, J. S., M. Brown, M. Dobosiewicz, I. G. Ishida, E. Z.
2 Macosko, *et al.*, 2016 Balancing selection shapes density-
3 dependent foraging behaviour. *Nature* **539**: 254–258.
4 Higgins, B. J. and D. Hirsh, 1977 Roller mutants of the nema-
5 tode *Caenorhabditis elegans*. *Molecular and General Genetics*
6 **MGG 150**: 63–72.
7 Hodgkin, J., 2005 Genetic suppression. *WormBook* .
8 Hodgkin, J. and T. Doniach, 1997 Natural variation and copu-
9 latory plug formation in *Caenorhabditis elegans*. *Genetics* **146**:
10 149–164.
11 Katoh, K., K.-i. Kuma, H. Toh, and T. Miyata, 2005 MAFFT
12 version 5: improvement in accuracy of multiple sequence
13 alignment. *Nucleic Acids Research* **33**: 511–518.
14 Kaur, T. and M. V. Rockman, 2014 Crossover heterogeneity in
15 the absence of hotspots in *Caenorhabditis elegans*. *Genetics* **196**:
16 137–148.
17 Kramer, J. M., 1994 Genetic Analysis of Extracellular Matrix in
18 *C. Elegans*. *Annual Review of Genetics* **28**: 95–116.
19 Kramer, J. M. and J. J. Johnson, 1993 Analysis of Mutations in the
20 Sqt-1 and Rol-6 Collagen Genes of *Caenorhabditis Elegans*.
21 *Genetics* **135**: 1035–1045.
22 Kramer, M., A.-L. Kranz, A. Su, L. H. Winterkorn, S. E. Albrit-
23 ton, *et al.*, 2015 Developmental Dynamics of X-Chromosome
24 Dosage Compensation by the DCC and H4K20me1 in *C. ele-*
25 *gans*. *PLoS Genetics* **11**.
26 Kusch, M. and R. S. Edgar, 1986 Genetic Studies of Unusual Loci
27 That Affect Body Shape of the Nematode *Caenorhabditis Ele-*
28 *gans* and May Code for Cuticle Structural Proteins. *Genetics*
29 **113**: 621–639.
30 Large, E. E., W. Xu, Y. Zhao, S. C. Brady, L. Long, *et al.*, 2016 Selec-
31 tion on a Subunit of the NURF Chromatin Remodeler Modifies
32 Life History Traits in a Domesticated Strain of *Caenorhabditis*
33 *elegans*. *PLOS Genetics* **12**: e1006219.
34 Li, H., 2011 A statistical framework for SNP calling, mutation
35 discovery, association mapping and population genetical pa-
36 rameter estimation from sequencing data. *Bioinformatics (Ox-*
37 *ford, England)* **27**: 2987–2993.
38 Li, H. and R. Durbin, 2010 Fast and accurate long-read align-
39 ment with Burrows-Wheeler transform. *Bioinformatics (Ox-*
40 *ford, England)* **26**: 589–595.
41 Madaan, U., E. Yzeiraj, M. Meade, J. F. Clark, C. A. Rushlow,
42 *et al.*, 2018 BMP Signaling Determines Body Size via Tran-
43 scriptional Regulation of Collagen Genes in *Caenorhabditis*
44 *elegans*. *Genetics* **210**: 1355–1367.
45 Mallard, F., L. Noble, T. Guzella, B. Afonso, C. F. Baer, *et al.*,
46 2019 Selection and drift determine phenotypic stasis despite
47 genetic divergence. *bioRxiv* p. 778282.
48 McGrath, P. T., M. V. Rockman, M. Zimmer, H. Jang, E. Z. Ma-
49 cosko, *et al.*, 2009 Quantitative mapping of a digenic behav-
50 ior trait implicates globin variation in *C. elegans* sensory
51 behaviors. *Neuron* **61**: 692–699.
52 McMahon, L., J. M. Muriel, B. Roberts, M. Quinn, and I. L. John-
53 stone, 2003 Two Sets of Interacting Collagens Form Function-
54 ally Distinct Substructures within a *Caenorhabditis elegans*
55 Extracellular Matrix. *Molecular Biology of the Cell* **14**: 1366–
56 1378.
57 Meyer, B. J. and L. P. Casson, 1986 *Caenorhabditis elegans* com-
58 pensates for the difference in X chromosome dosage between
59 the sexes by regulating transcript levels. *Cell* **47**: 871–881.
60 Noble, L. M., I. Chelo, T. Guzella, B. Afonso, D. D. Riccardi, *et al.*,
61 2017 Polygenicity and epistasis underlie fitness-proximal traits
62 in the *Caenorhabditis elegans* multiparental experimental evo-
lution (CeMEE) panel. *Genetics* pp. genetics–300406.
Noble, L. M., M. V. Rockman, and H. Teotónio, 2019 Gene-level
quantitative trait mapping in an expanded *C. elegans* multi-
parent experimental evolution panel. *bioRxiv* p. 589432.
Novelli, J., A. P. Page, and J. Hodgkin, 2006 The C Terminus
of Collagen SQT-3 Has Complex and Essential Functions in
Nematode Collagen Assembly. *Genetics* **172**: 2253–2267.
Nyström, J., Z.-Z. Shen, M. Aili, A. J. Flemming, A. Leroi, *et al.*,
2002 Increased or Decreased Levels of *Caenorhabditis elegans*
lon-3, a Gene Encoding a Collagen, Cause Reciprocal Changes
in Body Length. *Genetics* **161**: 83–97.
Paaby, A. B. and G. Gibson, 2016 Cryptic Genetic Variation in
Evolutionary Developmental Genetics. *Biology* **5**: 28.
Paaby, A. B. and M. V. Rockman, 2014 Cryptic genetic variation:
evolution’s hidden substrate. *Nature Reviews Genetics* **15**:
247–258.
Page, A. and I. L. Johnstone, 2007 The cuticle. *WormBook* .
Pagès, H., P. Aboyoun, R. Gentleman, and S. DebRoy, 2019
Biostrings: Efficient manipulation of biological strings.
Paradis, E. and K. Schliep, 2019 ape 5.0: an environment for
modern phylogenetics and evolutionary analyses in R. *Bioin-*
33 *formatics (Oxford, England)* **35**: 526–528.
Pebesma, E. J. and R. S. Bivand, 2005 Classes and methods for
spatial data in R. *R News* **5**: 9–13.
Persikov, A. V., J. A. M. Ramshaw, and B. Brodsky, 2005 Predic-
tion of Collagen Stability from Amino Acid Sequence. *Journal*
of *Biological Chemistry* **280**: 19343–19349.
Priess, J. R. and D. I. Hirsh, 1986 *Caenorhabditis elegans* mor-
phogenesis: the role of the cytoskeleton in elongation of the
embryo. *Developmental Biology* **117**: 156–173.
Roberts, B., C. Clucas, and I. L. Johnstone, 2003 Loss of SEC-
23 in *Caenorhabditis elegans* Causes Defects in Oogenesis,
Morphogenesis, and Extracellular Matrix Secretion. *Molecular*
Biology of the Cell **14**: 4414–4426.
Rockman, M. V. and L. Kruglyak, 2009 Recombinational land-
scape and population genomics of *Caenorhabditis elegans*. *PLOS*
Genetics **5**: e1000419.
Rockman, M. V., S. S. Skrovaneck, and L. Kruglyak, 2010 Selection
at linked sites shapes heritable phenotypic variation in *C.*
elegans. *Science (New York, N.Y.)* **330**: 372–376.
Scriver, C. R. and P. J. Waters, 1999 Monogenic traits are not
simple: lessons from phenylketonuria. *Trends in Genetics* **15**:
267–272.
Seidel, H. S., M. V. Rockman, and L. Kruglyak, 2008 Widespread
genetic incompatibility in *C. elegans* maintained by balancing
selection. *Science (New York, N.Y.)* **319**: 589–594.
Shephard, F., A. A. Adenle, L. A. Jacobson, and N. J. Szewczyk,
2011 Identification and functional clustering of genes regulat-
ing muscle protein degradation from amongst the known *C.*
elegans muscle mutants. *PLoS One* **6**: e24686.
Sterken, M. G., L. B. Snoek, J. E. Kammenga, and E. C. Andersen,
2015 The laboratory domestication of *Caenorhabditis elegans*.
Trends in genetics : TIG **31**: 224–231.
Summers, K. M., 1996 Relationship between genotype and phe-
notype in monogenic diseases: Relevance to polygenic dis-
eases. *Human Mutation* **7**: 283–293.
Swierczek, N. A., A. C. Giles, C. H. Rankin, and R. A. Kerr, 2011
High-throughput behavioral analysis in *C. elegans*. *Nature*
methods **8**: 592–598.
Teotónio, H., S. Carvalho, D. Manoel, M. Roque, and I. M. Chelo,
2012 Evolution of outcrossing in experimental populations of
Caenorhabditis elegans. *PLoS one* **7**: e35811.

- 1 Teuscher, A. C., E. Jongsma, M. N. Davis, C. Statzer, J. M.
2 Gebauer, *et al.*, 2019 The in-silico characterization of the
3 *Caenorhabditis elegans* matrixome and proposal of a novel
4 collagen classification. *Matrix Biology Plus* **1**: 100001.
- 5 van der Keyl, H., H. Kim, R. Espey, C. V. Oke, and M. K. Edwards,
6 1994 *Caenorhabditis elegans* *sqt-3* mutants have mutations in
7 the *col-1* collagen gene. *Developmental Dynamics: An Official*
8 *Publication of the American Association of Anatomists* **201**:
9 86–94.
- 10 Vu, V., A. J. Verster, M. Schertzberg, T. Chuluunbaatar, M. Spens-
11 ley, *et al.*, 2015 Natural Variation in Gene Expression Modu-
12 lates the Severity of Mutant Phenotypes. *Cell* **162**: 391–402.
- 13 Weber, K. P., S. De, I. Kozarewa, D. J. Turner, M. M. Babu,
14 *et al.*, 2010 Whole Genome Sequencing Highlights Genetic
15 Changes Associated with Laboratory Domestication of *C. elegans*. *PLOS ONE* **5**: e13922.
- 16 Webster, C. M., L. Wu, D. Douglas, and A. A. Soukas, 2013 A
17 non-canonical role for the *C. elegans* dosage compensation
18 complex in growth and metabolic regulation downstream
19 of TOR complex 2. *Development (Cambridge, England)* **140**:
20 3601–3612.
- 21 Westlund, B., L. W. Berry, and T. Schedl, 1997 Regulation of
22 Germline Proliferation in *Caenorhabditis Elegans*. In *Advances*
23 *in Developmental Biology (1992)*, edited by P. M. Wassarman,
24 volume 5, pp. 43–80, Academic Press.
- 25 Yang, J. and J. M. Kramer, 1999 Proteolytic Processing of
26 *Caenorhabditis elegans* SQT-1 Cuticle Collagen Is Inhibited
27 in Right Roller Mutants whereas Cross-linking Is Inhibited
28 in Left Roller Mutants. *Journal of Biological Chemistry* **274**:
29 32744–32749.
- 30 Yin, T., D. Cook, and M. Lawrence, 2012 *ggbio*: an R package for
31 extending the grammar of graphics for genomic data. *Genome*
32 *Biology* **13**: R77.
- 33 Yu, G., D. K. Smith, H. Zhu, Y. Guan, and T. T.-Y. Lam, 2017
34 *ggtree*: an r package for visualization and annotation of phy-
35 logenetic trees with their covariates and other associated data.
36 *Methods in Ecology and Evolution* **8**: 28–36.
- 37 Zamanian, M., D. E. Cook, S. Zdraljevic, S. C. Brady, D. Lee,
38 *et al.*, 2018 Discovery of genomic intervals that underlie nema-
39 tode responses to benzimidazoles. *PLOS Neglected Tropical*
40 *Diseases* **12**: e0006368.
- 41 Zhao, Y., L. Long, W. Xu, R. F. Campbell, E. E. Large, *et al.*,
42 2018 Changes to social feeding behaviors are not sufficient for
43 fitness gains of the *Caenorhabditis elegans* N2 reference strain.
44 *eLife* **7**: e38675.
- 45 Zych, K., B. L. Snoek, M. Elvin, M. Rodriguez, K. J. V. d. Velde,
46 *et al.*, 2017 *reGenotyper*: Detecting mislabeled samples in
47 genetic data. *PLOS ONE* **12**: e0171324.
- 48